Faraday Discussions d3fd00029j

We have presented the Graphical Abstract text and image for your article below. This brief summary of your work will appear in the contents pages of the issue in which your article appears.

PAPER

1

Kinetics of CN ($v = 1$) reactions with butadiene isomers at low temperature by cw-cavity ring-down in a pulsed Laval flow with theoretical modelling of rates and entrance channel branching

Shameemah Thawoos, Gregory E. Hall, Carlo Cavallotti and Arthur G. Suits*

Continuous-wave-cavity ring-down spectroscopy (CRDS) coupled with a pulsed uniform supersonic flow (Laval flow) are used to measure the reaction kinetics of the reaction of CN ($v = 1$) with 1,3- and 1,2-butadiene isomers at low temperature.

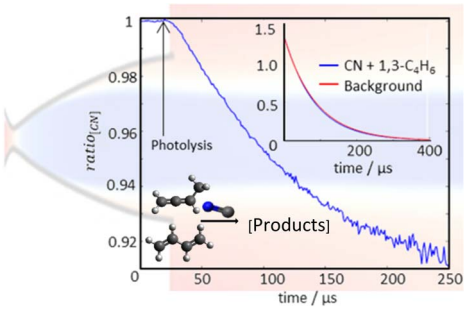

Please check this proof carefully. Our staff will not read it in detail after you have returned it.

Please send your corrections either as a copy of the proof PDF with electronic notes attached or as a list of corrections. **Do not edit the text within the PDF or send a revised manuscript** as we will not be able to apply your corrections. Corrections at this stage should be minor and not involve extensive changes.

Proof corrections must be returned as a single set of corrections, approved by all co-authors. No further corrections can be made after you have submitted your proof corrections as we will publish your article online as soon as possible after they are received.

Please ensure that:

- The spelling and format of all author names and affiliations are checked carefully. You can check how we have identified the authors' first and last names in the researcher information table on the next page. **Names will be indexed and cited as shown on the proof, so these must be correct.**
- Any funding bodies have been acknowledged appropriately and included both in the paper and in the funder information table on the next page.
- All of the editor's queries are answered.
- Any necessary attachments, such as updated images or ESI files, are provided.

Translation errors can occur during conversion to typesetting systems so you need to read the whole proof. In particular please check tables, equations, numerical data, figures and graphics, and references carefully.

Please return your **final** corrections, where possible within **48 hours** of receipt, by e-mail to: faraday@rsc.org. If you require more time, please notify us by email.

Funder information

Providing accurate funding information will enable us to help you comply with your funders' reporting mandates. Clear acknowledgement of funder support is an important consideration in funding evaluation and can increase your chances of securing funding in the future. We work closely with Crossref to make your research discoverable through the Funding Data search tool (http://search.crossref.org/funding).

Further information on how to acknowledge your funders can be found on our webpage (http://rsc.li/funding-info).

What is Funding Data?

Funding Data (http://www.crossref.org/fundingdata/) provides a reliable way to track the impact of the work that funders support. We collect funding information from our authors and match this information to funders listed in the Crossref Funder Registry. Once an article has been matched to its funders, it is discoverable through Crossref's search interface.

PubMed Central

Accurate funder information will also help us identify articles that are mandated to be deposited in PubMed Central (PMC) and deposit these on your behalf.

Providing funder information

We have combined the information you gave us on submission with the information in your acknowledgements. This will help ensure funding information is as complete as possible and matches funders listed in the Crossref Funder Registry. **Please check that the funder names and grant numbers in the table are correct.** This table will not be included in your final PDF but we will share the data with Crossref so that your article can be found *via* the Funding Data search tool.

Funder name	Funder's main country of origin	Funder ID (for RSC use only)	Award/grant number
National Science Foundation	United States	100000001	CHE-1955239
Ministero dell'Università e della Ricerca	Italy	501100021856	202082CE3T

Researcher information

Please check that the researcher information in the table below is correct, including the spelling and formatting of all author names, and that the authors' first, middle and last names have been correctly identified. **Names will be indexed and cited as shown on the proof, so these must be correct.**

If any authors have ORCID or ResearcherID details that are not listed below, please provide these with your proof corrections. Please ensure that the ORCID and ResearcherID details listed below have been assigned to the correct author. Authors should have their own unique ORCID iD and should not use another researcher's, as errors will delay publication.

Please also update your account on our online manuscript submission system to add your ORCID details, which will then be automatically included in all future submissions. See here for step-by-step instructions and more information on author identifiers.

First (given) and middle name(s)	Last (family) name(s)	ResearcherID	ORCID iD
Shameemah	Thawoos		
Gregory E.	Hall		0000-0002-8534-9783
Carlo	Cavallotti		
Arthur G.	Suits		0000-0001-5405-8361

Queries for the attention of the authors

Journal: **Faraday Discussions**

Paper: **d3fd00029j**

Title: **Kinetics of CN ($v = 1$) reactions with butadiene isomers at low temperature by cw-cavity ring-down in a pulsed Laval flow with theoretical modelling of rates and entrance channel branching**

For your information: You can cite this article before you receive notification of the page numbers by using the following format: (authors), Faraday Discuss., (year), DOI: 10.1039/d3fd00029j.

Editor's queries are marked on your proof like this **1**, **2**, etc. and for your convenience line numbers are indicated like this 5, 10, 15, …

Please ensure that all queries are answered when returning your proof corrections so that publication of your article is not delayed.

Query Reference	Query	Remarks
1	In the title and throughout, occurrences of "CN(v = 1)" and "CN(v = 0)" have been amended to "CN (v = 1)" and "CN (v = 0)", respectively, for consistency with how these terms appear elsewhere in the article. Please check that these changes are suitable.	
2	Have all of the author names been spelled and formatted correctly? Names will be indexed and cited as shown on the proof, so these must be correct. No late corrections can be made. Please tick this box or indicate your confirmation if you have no corrections to make to the proof ☐	
3	The sentence beginning "Indeed, the experimental rates measured for 1,3-butadiene…" has been modified for clarity. Please check that the changes are suitable and have not affected the meaning.	
4	In the Fig. 4 caption, references 29 and 31 are cited, however, the legend in the figure refers to the works of Morales and Butterfield, which appear in the reference list as ref. 25 and 26. Should the citations in the Fig. 4 caption be amended from "28, 29 and 31" to "25, 26 and 28"?	
5	In the Author contributions section, 'CAC' has been amended to 'CC' for consistency with the author list where 'Carlo Cavallotti' is listed without a middle initial. Please check that this change is suitable or indicate if any alternative changes are required.	
6	Have all of the funders of your work been fully and accurately acknowledged? Please tick this box or indicate your confirmation if you have no corrections to make to the proof ☐	
7	Ref. 13: Please provide the title/journal title and, if a journal article, page or article number(s).	

8	Ref. 16: Please provide the page (or article) number(s).	
9	Ref. 21: Please provide the title/journal title and, if a journal article, page or article number(s).	
10	Ref. 44: Please provide the page (or article) number(s).	
11	Ref. 46: Please provide the page (or article) number(s).	
12	Ref. 47: Please provide the title.	
13	Ref. 57: Please provide the DOI.	
14	Ref. 58: Please provide the DOI.	

Faraday Discussions

Cite this: DOI: 10.1039/d3fd00029j

PAPER

Kinetics of CN ($v = 1$) reactions with butadiene isomers at low temperature by cw-cavity ring-down in a pulsed Laval flow with theoretical modelling of rates and entrance channel branching

Shameemah Thawoos,[a] Gregory E. Hall,[b] Carlo Cavallotti[c] and Arthur G. Suits *[a]

Received 6th February 2023, Accepted 16th March 2023

DOI: 10.1039/d3fd00029j

We present an experimental and theoretical investigation of the reaction of vibrationally excited CN ($v = 1$) with isomers of butadiene at low temperature. The experiments were conducted using the newly built apparatus, UF-CRDS, which couples near-infrared cw-cavity ring-down spectroscopy with a pulsed Laval flow. The well-matched hydrodynamic time and long ring-down time decays allow measurement of the kinetics of the reactions within a single trace of a ring-down decay, termed Simultaneous Kinetics and Ring-down (SKaR). The pulsed experiments were carried out using a Laval nozzle designed for the 70 K uniform flow with nitrogen as the carrier gas. The measured bimolecular rates for the reactions of CN ($v = 1$) with 1,3-butadiene and 1,2-butadiene are $(3.96 \pm 0.28) \times 10^{-10}$ and $(3.06 \pm 0.35) \times 10^{-10}$ cm^3 per molecule per s, respectively. The reaction rate measured for CN ($v = 1$) with the 1,3-butadiene isomer is in good agreement with the rate previously reported for the reaction with ground state CN ($v = 0$) under similar conditions. We report the rate of the reaction of CN ($v = 1$) with the 1,2-butadiene isomer here for the first time. The experimental results were interpreted with the aid of variable reaction-coordinate transition-state theory calculations to determine rates and branching of the addition channels based on a high-level multireference treatment of the potential energy surface. H-abstraction reaction rates were also theoretically determined. For the 1,2-butadiene system, theoretical estimates are then combined with literature values for the energy-dependent product yields from the initial adducts to predict overall temperature-dependent product branching. H loss giving 2-cyano-1,3-butadiene + H is the main product channel, exclusive of abstraction, at all energies, but methyl loss forming 1-cyano-prop-3-yne is 15% at low temperature growing to 35% at 500 K. Abstraction forming HCN and various radicals is important at 500 K and above. The astrochemical implications of these results are discussed.

[a]*Department of Chemistry, University of Missouri, Columbia, MO 65211, USA. E-mail: Suitsa@missouri.edu*

[b]*Chemistry Division, Brookhaven National Laboratory, Upton, NY 11973, USA*

[c]*Department of Chemistry, Materials, and Chemical Engineering "G. Natta", Politecnico di Milano, Milano 20133, Italy*

Introduction

The recent identification of benzonitrile, as well as the first branched alkyl species, isopropyl cyanide, in interstellar environments has propelled interest in understanding reactions leading to nitrogen-rich complex molecules at low temperatures.[1–8] The interstellar medium (ISM) and planetary atmospheres such as that of Titan are both rich in neutral molecules including cyano radicals (CN) and a variety of hydrocarbons. Reactions of CN with unsaturated hydrocarbons can be a key aspect of the growth of small molecules into nitrogen-containing complex organic molecules. Although the temperatures and densities are very different in these different environments, understanding pathways that contribute to such products at low temperature is essential to permit predictions of the temperature-dependent product branching, which will have a significant impact on the chemistry downstream, and is of great fundamental chemical interest as well.

The CRESU technique (a French acronym for reaction kinetics in uniform supersonic flows) has opened up experimental investigation of such reactions in laboratory settings at temperatures of interstellar molecular clouds and planetary atmospheres.[9–13] The CRESU technique creates a "wall-less" reactor at temperatures as low as 15 K by creating uniform supersonic expansion.[14–16] The uniform supersonic flow is achieved by expanding a gas from a high-pressure stagnation reservoir to a low-pressure reaction chamber through a convergent-divergent nozzle commonly known as a Laval nozzle.[9,17] Most of the CRESU work has been performed using laser-induced fluorescence (LIF) detection, which is very sensitive and well-suited to the flow environment. However, there is a rather limited range of species amenable to LIF detection. Recent work in our group and others has expanded the range of detection techniques for application in the supersonic flow environment, including chirped-pulse microwave spectroscopy, VUV photoionization, and VUV-LIF.[18–22] Another recent development from our group has been the implementation of cw-cavity ring-down spectroscopy in the uniform flow (UF-CRDS). As we have recently shown, the hydrodynamic time in the flow is well-matched to the ring-down decay, so that with this approach we can record the full kinetic trace on each 100 μs ring-down, a method termed Simultaneous Kinetics and Ring-down (SKaR).[23] Here we report rates of the reactions of vibrationally excited CN ($v = 1$) with butadiene isomers at 70 K using the UF-CRDS method with SKaR.[24] We combine this experimental investigation with high-level *ab initio* calculations and transition-state theory modeling to interpret the observations.

Theoretical investigations of low-temperature CN radical reactions and their experimental study through advances in spectroscopic detection methods coupled with CRESU[24–26] have provided a solid basis for considering these reactions as a major contributor to the formation of nitrogen-rich compounds in astrochemical environments.[25] Experimental and theoretical findings for reactions of ground-state CN with isomers 1,2-butadiene and 1,3-butadiene suggest the CN adds without a barrier to form long-lived C_5H_6N complexes leading to a range of possible products.[25,27] The results of crossed-molecular beam studies conducted under single collision conditions and supported by electronic-structure calculations suggest a nearly exclusive formation of the

ART ■ D3FD00029J

thermodynamically less favorable product isomer 1-cyano-1,3-butadiene with minor branching to pyridinyl radicals,[25] although it is not clear whether addition to the C2 carbon giving 2-cyano-1,3-butadiene was considered (*vide infra*). The rates for the reaction of 1,3-butadiene with CN ($v = 0$) have been reported for a wide range of temperatures ranging from 1200 K (ref. 26 and 28) to as low as 23 K.[25] The rates measured above room temperature by both Butterfield *et al.*[26] and Gardez *et al.*[28] show a negative temperature dependence, while the experiments conducted at temperatures lower than room temperature using the CRESU apparatus by Morales *et al.*[25] show a fast reaction with a mild positive temperature dependence and good agreement for the room-temperature rate. In contrast, no experimental measurement of the rate of reaction of CN with 1,2-butadiene has been reported to our knowledge. However, theoretical studies carried out by Jamal *et al.*[27] for the reaction between CN and 1,2-butadiene predicts it can proceed *via* CN addition (to the C^1, C^2 or C^3 carbon, or insertion into the C=C double bonds) or by H abstraction either directly or *via* a CN roaming mechanism. This can be followed by H loss mainly giving 2-cyano-1,3-butadiene, or by methyl loss giving either 1-cyano-prop-3-yne or cyanoallene, with the relative yields sensitive to the nature of the initial adduct. They suggested the dominant product from the CN reaction with 1,2-butadiene is 2-cyano-1,3-butadiene + H, which arises from the pathway leading to CN addition to the C^2 carbon atom, but we will investigate this more closely below.

Experimental methods

The experiments were performed using the UF-CRDS apparatus.[24] In brief, the UF-CRDS apparatus is a home-built instrument that couples a highly sensitive near-infrared continuous-wave cavity ring-down spectrometer (cw-CRDS) with a pulsed Laval flow. The CRD spectrometer consists of two high-reflectivity plano-concave mirrors (reflectivity at 7070 cm^{-1} is 99.9965%) separated by 80 cm. A distributed feedback (DFB) diode laser centered at 7070 cm^{-1} is used as the laser source to probe the rotational levels of CN ($v = 1$). The laser output is fiber-coupled and most of it is sent through an acoustic optical modulator (AOM), which acts as a fast switch interrupting the laser input and allowing ring-down events. About 10% of the output is sent to a wavemeter that monitors the wavelength continuously. The output laser from the AOM is steered into the cavity using two steering mirrors and a mode-matching lens. The output cavity mirror is mounted on a piezoelectric transducer, which allows the cavity length modulation at a set frequency and amplitude. The transmitted light at the output high-reflectivity mirror of the cavity is focused on to a InGaAs photodiode. All timing, triggering, monitoring, and data storage are done using a multi-function DAQ board and a custom-built LabVIEW code.

The CRD spectrometer is mounted perpendicular to the pulsed Laval flow. The pulsed Laval flow is generated using a home-built, high-throughput piezoelectric stack valve[29] and a 3D printed Laval nozzle. The stack valve rapidly fills up a reservoir of approximately 20 cm^3, and the gas is allowed to expand through a Laval nozzle into a vacuum chamber that is pumped by a turbomolecular pump backed by a dry roots pump. The stack valve, the reservoir, and the Laval nozzle are mounted on a motorized translational stage that could be moved vertically and horizontally. This allows us to move the Laval nozzle with respect to the

stationary CRDS and a pitot probe. The pulsed flow generated is characterized using a two-dimensional pitot map, as well as spectroscopic measurements conducted in the flow. In the present study, a nominally 70 K 3D printed Laval nozzle is used. The temperature measured in the isentropic core using the pitot probe was 68 ± 2 K, and the temperature retrieved using a Boltzmann distribution plot from the spectra recorded for acetylene overtone ($1_0^2 5_0^1$) was 66 ± 6 K.[24]

Previously reported timing and data acquisition were adopted based on the method introduced by Hippler *et al.*[30] and implemented successfully by many others.[31–34] However, this method was quite susceptible to environmental changes such as vibrations and temperature causing it to skip cavity resonances or drift with respect to the modulation frequency. This limited the throughput of the data acquisition. Thus, a revised version of the cavity modulation and data acquisition was implemented, which will be described in greater detail in a future publication. In brief, the triangular voltage modulation was replaced with sinusoidal voltage modulation. An independent servo feedback loop was implemented to adjust the DC bias for the cavity modulation drive to keep the modulation cycle centered on one transmission fringe, eliminating slow drift of fringe timing. The cavity is modulated at a fixed 50 Hz frequency. The 50 Hz sinusoidal signal and a phase-synchronized timing pulse at a selected, reduced repetition rate for the pulsed flow and excimer photolysis were generated continuously. The pulsed Laval flow is generated using the piezoelectric stack valve, which is held open for 3 ms. The phase for the synchronization pulse is chosen such that the next fringe after the trigger will occur near the central, most uniform portion of the gas pulse. The cavity transmission is monitored constantly by a photodiode. When the signal exceeds a threshold, a trigger pulse is sent to the control input of the radio frequency driver for the AOM, interrupting the injection of resonant laser light into the cavity and initiating a ring-down event. A 400 μs ring-down signal is recorded at 1 MHz sampling rate. The excimer laser is fired to initiate photochemistry at the same rate as the pulsed flow, at a selected time interval (23 μs) after the onset of the first ring-down acquisition following the piezo stack trigger. The delayed photolysis provides a pre-trigger ring-down signal for normalization, in addition to the reference ring-down signals, repeatedly measured during the intervals between successive gas pulses. The precise elapsed time between the stack trigger and the optical triggering at the beginning of the next ring-down fringe is measured and used to accumulate averages of the ring-down data in bins of 200 μs width. When analyzing the CN kinetics, the ring-down events are averaged for two time bins (400 μs) centered within the gas pulse.

High purity ≥ 99.0% 1,3-butadiene ($CH_2CHCHCH_2$) and 97% cyanogen bromide (BrCN) were purchased from Sigma-Aldrich, 98% 1,2-butadiene (CH_2-$CCHCH_3$) was purchased from ChemSampCo, Inc., and ultra-high purity nitrogen gas was purchased from Airgas. All the chemicals are used without further purification. BrCN was used as the source of vibrationally excited CN ($v = 1$) and the radicals were produced by photolyzing the flow mixture containing BrCN using an excimer laser operated at 248 nm. Photolysis of BrCN has been studied extensively and the literature suggests that the vibrational excitation is higher in 248 nm photodissociation of BrCN compared to that at 193 nm.[35–39] The 248 nm excimer was operated at an average power of 75 mJ per pulse and the laser fluence at the exit of the nozzle is approximately 133 mJ cm^{-2}. The excimer is aligned along the axis of the nozzle and counter-propagates to the flow. To maximize the overlap of

the CRDS probing region and the photolysis volume, the rectangular shape of the excimer is rotated using a periscope and loosely focused vertically using a 2 m focal length cylindrical lens. This creates a nearly uniform column of CN ($v = 1$) that is rapidly rotationally cooled to the flow temperature and reacts with the diene that is co-seeded in the flow. The BrCN concentration is set such that the maximum estimated CN produced was 2.7×10^{11} molecule per cm^3. This reacting column of gas passes by the probe region where it is detected by CRDS. The rate of reaction is measured by monitoring the loss of CN ($v = 1$) by tuning the DFB diode laser at 7070.240 cm^{-1} ($j = 5.5$), R1 branch of the CN ($v = 1$) electronic transition $A^2\Pi$–$X^2\sum^+$. The entire course of the reaction is monitored during each ring-down pulse, and this is repeated and averaged over ~1200 gas pulses or ~5 minutes at each concentration of the co-reactant.

Experimental results

The measurement of rates of reaction is accomplished by a method described by Brown *et al.*,[23] referred to as SKaR (Simultaneous Kinetics and Ring-down). In the absence of the photolysis pulse and the intra-cavity absorption by CN radicals, the measured ring-down signal is a single-exponential decay with a time constant τ_0. When there is a time-dependent concentration of a resonant absorber inside the cavity, the instantaneous ring-down rate is accelerated relative to the empty cavity, leading to a faster, non-exponential decay that depends on the time-dependent concentration of the absorber, $[A](t)$ according to eqn (1).[23]

$$I(t) = I_0 \exp\left[-c\sigma \frac{L_a}{L} \int_0^t [A](t)\mathrm{d}t - \frac{t}{\tau_0} \right] \quad (1)$$

Here I_0 is the intensity at time zero, c is the speed of light, σ is the absorption cross section of the absorbing species, and $\frac{L_a}{L}$ is the ratio of the absorbing path length to the total cavity length. The dependence on the empty cavity ring-down is removed by computing the ratio of $I(t)$ to the empty-cavity ring-down signal:

$$\mathrm{Ratio}(t) = \frac{I(t)}{I_0\, \mathrm{e}^{-t/\tau_0}} = \exp\left[-c\sigma \frac{L_a}{L} \int_0^t [A](t)\mathrm{d}t \right] \quad (2)$$

The time-dependent concentration can then be formally obtained by differentiating the logarithm of the ratio:

$$[A](t) = \frac{-1}{c\sigma} \frac{L}{L_a} \frac{\mathrm{d}\ln[\mathrm{ratio}(t)]}{\mathrm{d}t} \quad (3)$$

No explicit functional form for the time dependence need be assumed to transform the measured ring-down signals to a kinetic trace with eqn (3), although ratio(t) becomes increasingly poorly determined as the ring-down decay proceeds, and the numerical derivative amplifies the noise, as discussed by Brown *et al.*[23] The time-dependent signal attributable to the absorption of CN ($v = 1$) in selected low rotational states is empirically found to follow a sequential growth and decay model of the form

$$[\mathrm{CN}](t) = a(\mathrm{e}^{-k_1 t} - \mathrm{e}^{-k_2 t}) \quad (4)$$

where a is an adjustable amplitude, the rise rate k_2 qualitatively accounts for the rotational thermalization of the initially hot (and unobserved) rotational states of CN ($v = 1$) formed in the photolysis of BrCN,[38,40] and the fall-rate k_1 is nearly negligible in the absence of the hydrocarbon reactant, but increases linearly with added hydrocarbon.

Fig. 1A shows an example of the background-ring-down-corrected ratio(t) for CN ($v = 1$, and $J = 5.5$) in the presence of 1,3-butadiene in a 70 K flow. The inset to Fig. 1A shows the averaged foreground and background ring-down signals used to compute this ratio. In Fig. 1B, the blue trace is derived from the numerical derivative of the logarithm of the ratio. In practice, the fit is performed by adjusting parameters a, k_1 and k_2 in eqn (4), while minimizing the squared error in the integrated form of eqn (2), when compared directly to the experimentally determined ratio(t), thus avoiding the numerical differentiation step in the analysis. The red line fit in Fig. 1B is the rise–fall function from eqn (4) that produces the best fit to the ratio in a time window from the time of photolysis at $t = 23$ μs until $t = 180$ μs.

Measurements were performed with incremental additions of 1,3- or 1,2-butadiene, with reaction conditions as summarized in Table 1. Concentrations of the added hydrocarbons were small enough to avoid significant perturbation to the flow conditions, but high enough to ensure pseudo-first-order conditions, in large excess over the photolytic CN radical concentration.

Fig. 2A and B illustrate the variation of the rise–fall fits with changing concentrations of added 1,3-butadiene and 1,2-butadiene, respectively, in a 70 K flow. The rise rates are nearly independent of the added hydrocarbon, and the peak concentrations of CN ($v = 1$, and $J = 5.5$) occur about 20 μs after laser photolysis in all cases. The decay rates k_1 increase linearly with the added hydrocarbon concentration, as plotted in Fig. 2C and D, according to eqn (5):

$$k_1 = k_b[\mathrm{C_4H_6}] + k_0 \quad (5)$$

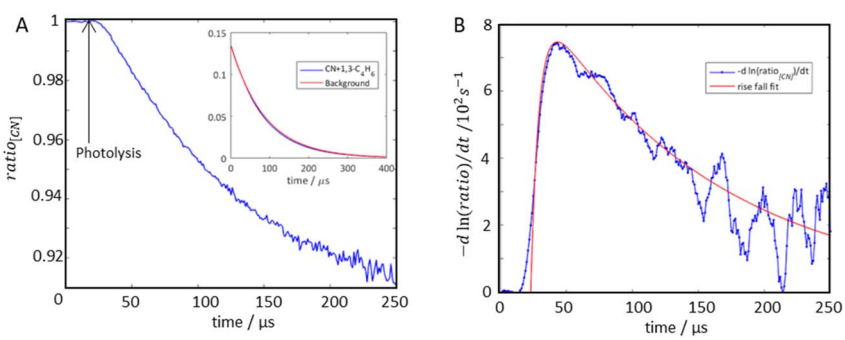

Fig. 1 (A) Background normalized ring-down decay. Inset: Background ring-down (red), ring-down with the absorber, CN ($v = 1$) in the presence of 1,3-butadiene. Arrow indicates when the photolysis laser is fired. (B) Negative derivative of the natural logarithm of the smoothed data from (A) (blue) and the rise–fall fit (red) where the time limits are set at 23 and 180 μs for the lower and upper limits, respectively.

Table 1 Summary of reaction flow conditions and rates obtained for the reaction CN ($v = 1$) + isomers of butadiene

Isomer	Gas	Flow density/10^{16} molecules per cm^3	Range of [C_4H_6]/10^{13} molecules per cm^3	No. of measurements	Rate/10^{-10} cm^3 per molecule per s
1,2-Butadiene	N_2	5.5	0.81–6.52	7	3.06 ± 0.35
1,3-Butadiene	N_2	5.5	1.42–7.07	7	3.96 ± 0.28

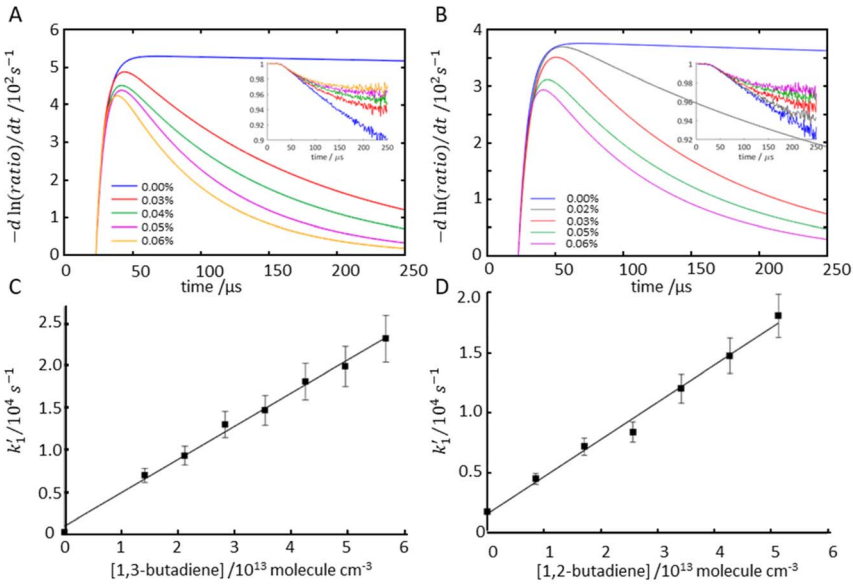

Fig. 2 Selected rise–fall fit for varying (A) 1,3-butadiene and (B) 1,2-butadiene densities. Insets: The respective background normalized ring-down ratio traces. The percent butadiene isomer added is the percent fraction of the flow density, 5.5 × 10^{16} molecules per cm^3. (C) and (D) are respective bimolecular rate plots for pseudo first-order rate *vs.* 1,3 and 1,2 butadiene isomer densities.

The intercept k_0 is the first-order rate of loss of CN ($v = 1$) in the absence of co-reactant, likely from side reactions or diffusion of CN ($v = 1$) from the probe region. We have observed a significant dependence of k_0 on excimer alignment along the axis of the flow. The slope from Fig. 2C gives a bimolecular rate $k_{1,3}$ for 1,3-butadiene of 3.96 ± 0.28 ×10^{-10} cm^3 per molecule per s at 70 K. The rate reported by Morales *et al.*[25] for the reaction of CN ($v = 0$) with 1,3-butadiene at 70 K is in good agreement with our present measurement, suggesting the low temperature rate of the reaction of CN with 1,3-butadiene has little if any dependence on the vibrational excitation of the CN radical. The rate measured for the reaction of CN ($v = 1$) with the 1,2-butadiene isomer ($k_{1,2}$) at 70 K is 3.06 ± 0.35 × 10^{-10} cm^3 per molecule per s (Fig. 2B and D). This is significantly

slower than the corresponding rate for the 1,3 isomer. The uncertainty given is at the 95% confidence interval and is dominated by uncertainties in the fits to the first-order decay rates and estimated from the reproducibility of replicate measurements.

Theoretical methods

The rate constants of the entrance and H-abstraction channels of the reaction between CN, 1,2-butadiene and 1,3-butadiene were theoretically determined. Simulations were performed for CN ($v = 0$) as it was assumed that the CN vibrational excitation energy does not contribute to the system reactivity. This means that the population of the density of states at the transition state is considered to be adiabatic with respect to the CN vibrational excitation. This assumption is supported by experimental evidence, which shows that the rate constants for the reaction of CN ($v = 0$) and CN ($v = 1$) are in good agreement for 1,3-butadiene where both measurements have been made. Total rate constants were determined as the sum of contributions from central (two separate sites in the case of 1,2-butadiene, one for 1,3-butadiene) and terminal carbon atom additions, as well as from H-abstraction from all possible sites.

Addition reactions were investigated using variable reaction-coordinate transition-state theory (VRC-TST)[41] to determine reactive fluxes at short and long ranges for each examined reaction channel. The addition rate constant was then computed through a master equation (ME) simulation using the two-transition-state model,[42] which allows determination of a phenomenological rate constant for a system whose reactivity is controlled by the presence of two bottlenecks along the reaction pathway. VRC-TST simulations were performed using the partially automated protocol that is implemented in EStokTP.[43,44] In short-range simulations, pivot atoms are placed along the axis of the bond that is established between the reactants in the minimum-energy structure formed when the fragments are at a 2.4 Å separation and displaced with respect to the reactive centers by 0.001, 0.1, and 0.2 Bohr. Two pivot points are used for butadiene and one for CN, centered on the carbon atom. To restrict the stochastic sampling performed in VRC-TST simulations to the investigated addition site, repulsive potentials were placed on the competitive reaction sites. This is expected to give results equal to those that can be obtained using multifaceted dividing surfaces placing pivot points on each competitive reactive site.[41] Interaction potentials between the fragments were determined on CASPT2(5e,5o)/dz geometries at the CASPT2(11e,10o) level with energies computed with the aug-cc-pVTZ and aug-cc-pVQZ basis sets and extrapolated to the complete basis set limit. VRC-TST simulations were performed at the CASPT2(5e,5o)/dz level using correction potentials for geometry relaxation and high-level energy extrapolation.

Phenomenological rate constants for H-abstraction reactions were determined with the *ab initio* transition-state theory-based master equation approach (AITSTME,[45]), using the automated 1TS model implemented in EStokTP.[43] Geometries and Hessians at the saddle points were determined at the ωB97X-D/jun-cc-pVTZ level, and energies at the CCSD(T) level extrapolated to the complete basis set.[46] A 1D hindered rotor model was used for butadiene internal torsions.

ART ■ D3FD00029J

Three different H-abstraction reaction channels were investigated for both 1,2-butadiene and 1,3-butadiene.

Density functional theory simulations were performed using Gaussian 09,[47] CASPT2 and CCSD(T) calculations with Molpro,[48] and ME simulations with MESS.[49]

Computational results

The rate of addition of CN to butadiene is controlled by two dynamic bottlenecks, located at long and short ranges. Short-range interactions control the reactive flux at high temperatures, while at the temperature of the present experiments, 70 K, long-range interactions are dominant over short-range interactions. The potential energy surfaces (PESs) for the addition and abstraction processes for CN ($v = 0$) + 1,3-butadiene and CN ($v = 0$) + 1,2-butadiene are shown in Fig. 3A and B, respectively.

The total rate constants were multiplied by correction factors of 0.9 and 0.8 to account for recrossing, which is not included in VRC-TST. Though there is some uncertainty in this parameter, which is often system dependent,[45] a good fit is usually obtained using recrossing coefficients of 0.8–0.9. Indeed, the experimental rates measured for 1,3-butadiene, shown in Fig. 4, are in excellent agreement when the recrossing coefficient is set to 0.8, while those for 1,2-butadiene measured in this work agree well when using a recrossing coefficient of 0.9, as shown in Fig. 5. It can also be seen that the total rate constant for the reaction between CN and 1,3-butadiene is well described by the theoretical model for the whole range of temperatures for which experimental data are available. The contributions of the different channels to the total rate constant reported in Fig. 4 and 5 highlight that the most reactive site for addition at low temperatures is the terminal site for 1,3-butadiene and the C2 site for 1,2-butadiene. This is consistent with the PESs of the two reactive systems, as the fastest channels are also the most exothermic. As can be seen, up to about 1000 K, the dominant reaction channel is addition, after which abstraction starts gaining relevance.

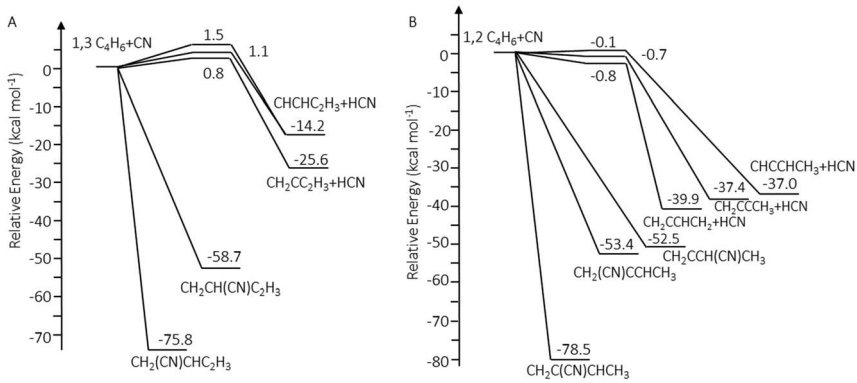

Fig. 3 Calculated PESs for the reaction between CN ($v = 0$) and 1,3-butadiene (A) and 1,2-butadiene (B). Energies are reported in kcal mol^{-1} and include zero-point energy corrections.

ART ■ D3FD00029J

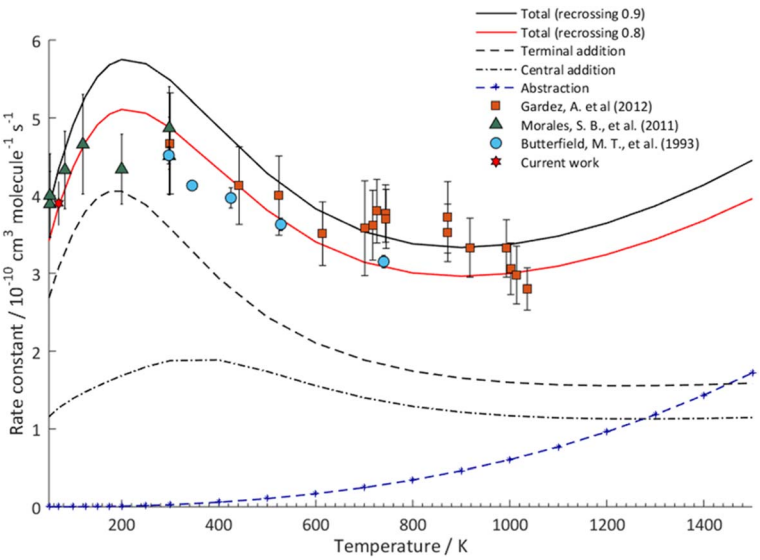

Fig. 4 Comparison between calculated and experimental data (ref. 28, 29, 31, and the present study) for the total rate constant for the reaction between 1,3-C_4H_6 and CN.

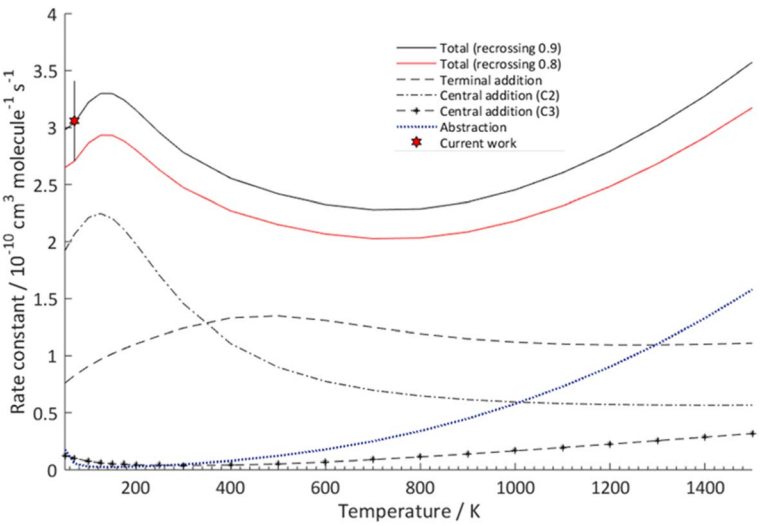

Fig. 5 Comparison between the calculated and experimental rate constant measured in the present work for the reaction between 1,2-C_4H_6 and CN.

Discussion

It is evident that the reactions of CN ($v = 1$) with both butadiene isomers at 70 K are quite fast and the reaction with the 1,3 isomer is significantly faster than the 1,2 isomer ($k_{1,3}/k_{1,2}$ is 1.29). Although the conjugated 1,3-butadiene is more than 50 kJ mol^{-1} lower in energy than 1,2 butadiene, it has two accessible terminal

ART ■ D3FD00029J

sites for addition that can produce conjugated products. These terminal sites are more reactive, and this can contribute to the long-range attraction important at low temperature. Both reactions presented here are believed to be candidates leading to the formation of pyridine, the nitrogen-containing aromatic analog to benzene. However, both quantum chemical calculations[27,50] and crossed molecular beam experiments[50] suggested that the only reaction that possibly could lead to pyridine is the reaction with the 1,3 isomer. However, the reaction with the 1,3 isomer mainly produced the thermodynamically less favorable linear 1-cyano-1,3-butadiene ($CH(CN)CHC_2H_3$) product[25] with branching to pyridine predicted to be less than 0.2% and likely much lower. This is an interesting contrast to the reaction of the isoelectronic CCH radical with 1,3-butadiene, which gives a significant yield of benzene. The difference is chiefly attributed to the much greater stability of the initial adduct in the CCH case.

As noted in the introduction, however, the prediction above assumed solely CN addition to the terminal carbon. Our results examining the entrance channel in detail show significant branching to central addition in 1,3-butadiene: about 25% at 70 K and over 50% at 300 K and above. The subsequent fate of the central addition intermediate is not clear, however, as that region of the PES and subsequent dynamics were not investigated by Morales *et al.*, nor by us. Earlier theoretical treatment by Sun *et al.*[51] suggested that the intermediate formed by C2 addition would isomerize to the C1 adduct, so perhaps this is why C2 addition was neglected. In any case, formation of pyridine from the C2 adduct seems even less likely than from the terminal addition adduct, so the implications for the low-pressure product branching, insofar as pyridine is concerned, are likely unchanged. In any case, this is an interesting subject for further investigation.

For the CN + 1,2-butadiene reaction, although there are no reported experimental studies, there is an analogous theoretical investigation conducted by Jamal and Mebel.[27] For this system, they have performed a detailed investigation of the energy-dependent branching starting from the intermediates formed from addition at the C1, C2, or C3 carbons or by insertion into the double bonds, but without knowing the weighting of the initial addition or abstraction. The product channels predicted by Jamal and Mebel include 1-cyano-prop-3-yne ($CH_2(CN)CCH$) + CH_3 (P1), 2-cyano-1,3-butadiene ($CH_2C(CN)C_2H_3$) + H (P2), and cyanoallene ($CH_2CCH(CN)$) + CH_3 (P3). We can combine our results for the branching of the initial addition step and abstraction with theirs for the decay from the various intermediates to predict the overall branching. The results are presented in Table 2.

Table 2 Temperature-dependent branching (%) for the indicated product channels (see text) combining the present entrance channel branching with calculations of product branching arising from C1, C2 or C3 addition from ref. 30. We take their 0 K value at 50 K and use 1 kcal $mol^{-1} \approx 500$ K. H abstraction is summed over all H atom sites

T (K)	P1	P2	P3	Abstraction
50	15	78	1	6
500	35	60	1	4
1000	30	44	3	24
1500	21	31	4	44

ART ■ D3FD00029J

At low temperature, CN addition at the C2 carbon is favored nearly 3:1 over the terminal site. According to Jamal and Mebel, C2 addition leads exclusively to the H-loss channel, P2, while addition at the terminal site branches 3:2 for P1 and P2, respectively. As a result, H loss is strongly favored at low temperature. As the temperature is increased, addition at the terminal carbon grows in importance, exceeding that at C2 at around 350 K. At 500 K, C1 is favored over C2 56:33 so that branching to P1 reaches 35%. Abstraction is still almost negligible. As the temperature is further increased, C1 addition continues to grow in importance, and abstraction also comes into play reaching 31% at 1000 K and 41% at 1500 K. H loss is always the dominant product of addition, but still, it is only 60% at 500 K and 31% at 1500 K. Addition at C3 is always minor but increases with temperature, reaching 9% at 1500 K. As this is the only pathway to cyanoallene (P3), this channel never exceeds 4%.

Although the present results are consistent with earlier conclusions that pyridine formation is unlikely in these reactions, the fast reaction rates and the dominance of CN-substituted unsaturated products formed implies the above reactions could be prominent elementary steps in systematic growth of more complex nitrogen-containing compounds detected in the ISM.[1–4,52,53] Although differing in density and collision frequency by many orders of magnitude, these same reactions are certainly important in the chemistry of planetary atmospheres, such as that of Titan, which possess rich chemistry driven by energetic processing of the dense N_2–CH_4 atmosphere.[54–56] Nitriles and unsaturated hydrocarbons are abundant, leading to the formation of aerosol haze layers that have been the subject of intense investigation for decades, while analogous hazes on exoplanets frustrate interrogation of their atmospheres.[57,58] Understanding the barrierless CN addition reactions studied here is part of the ongoing effort to unravel the detailed chemistry of these hazes. Another fascinating aspect of Titan chemistry is its "cryominerology", rocks comprising butadiene, HCN and other species formed as the hazes rain down on the surface.[59,60] Understanding formation of these extraordinary minerals will also benefit from this effort.

As noted in the introduction, isopropyl cyanide was the first branched-chain alkyl species detected in the ISM, following 5 years after detection of the normal species.[8] Modeling shows distinct formation pathways for each. The initial modeling ascribed iso-formation to the CN reaction with 2-propyl radicals in ice mantles, while *n*-propyl cyanide was formed by ethyl radical reaction with CH_2CN. The iso species is now attributed to methyl addition to CH_3CHCN, with the latter formed by CN reaction with ethylene in the ice.[61] In the newer models, the normal species is still formed largely by the same pathway, but CN + propene is also found to play a major role. However, the model restricts branching in that reaction exclusively to *n*-propyl cyanide, otherwise it is found difficult to account for the predominance of the normal isomer.[62] The nature of the initial addition site is thus critical in determining the branching downstream. As we have shown, the temperature dependence of the addition site and addition *vs.* abstraction can vary strongly with temperature.

Conclusions

We have studied the kinetics of the reaction of CN ($v = 1$) with 1,2- and 1,3-butadiene at 70 K in a pulsed Laval flow under pseudo-first order conditions. The

ART ■ D3FD00029J

density of the reactant CN was monitored using cw-CRDS in the near-IR using the SKaR technique. Both reactions were fast, but that with 1,3-butadiene was significantly faster: $(3.96 \pm 0.28) \times 10^{-10}$ and $(3.06 \pm 0.35) \times 10^{-10}$ cm^3 per molecule per s for 1,3- and 1,2-butadiene, respectively. The results were interpreted with the aid of VRC-TST calculations of the entrance channel branching based on multireference *ab initio* calculations of the initially formed adducts, which gave good agreement with the measured rates. The theoretical prediction of the initial adduct formation was combined with previous Rice–Ramsperger–Kassel–Marcus (RRKM) calculations of the subsequent product yields to predict overall product branching. At low temperature, H loss forming 2-cyano-1,3-butadiene is the dominant product as a result of addition at C2, but CH_3 + 1-cyano-prop-3-yne following addition at C1 is also significant and grows in importance with temperature. Addition at C3 is always minor and, as a result, the cyanoallene + CH_3 product channel yield is less than 4%. Abstraction contributes a few percent at low temperature, increasing to 44% at 1500 K.

Data availability

Master equation inputs for all the reactions studied, as well as all the details on stationary points and VRC-TST fluxes necessary to reproduce the simulations are available at **https://doi.org/10.5281/zenodo.7695851**.

Author contributions

AGS conceived the experiment. ST carried out all experiments, GEH conceived the data acquisition and analysis protocol, and GEH and ST implemented it. CC conceived and performed all theoretical calculations. ST and AGS wrote the paper with contributions from all authors.

Conflicts of interest

There are no conflicts to declare.

Acknowledgements

This work was supported by the NSF under award number CHE-1955239 and by the Italian MUR (PRIN 2020 – Grant 202082CE3T). CC acknowledges the CINECA award HP10BCGTXF, under the ISCRA initiative, for the availability of high-performance computing resources and support. The contributions of GEH, as a senior scientist emeritus at BNL, have not been directly supported by any specific BNL or DOE funded program.

Notes and references

1 B. A. McGuire, A. M. Burkhardt, S. Kalenskii, C. N. Shingledecker, A. J. Remijan, E. Herbst and M. C. McCarthy, *Science*, 2018, **359**, 202–205.

2 M. C. McCarthy, K. L. K. Lee, R. A. Loomis, A. M. Burkhardt, C. N. Shingledecker, S. B. Charnley, M. A. Cordiner, E. Herbst, S. Kalenskii and E. R. Willis, *Nat. Astron.*, 2021, **5**, 176–180.

3 B. A. McGuire, R. A. Loomis, A. M. Burkhardt, K. L. K. Lee, C. N. Shingledecker, S. B. Charnley, I. R. Cooke, M. A. Cordiner, E. Herbst and S. Kalenskii, *Science*, 2021, **371**, 1265–1269.

4 A. Belloche, R. Garrod, H. Müller, K. Menten, C. Comito and P. Schilke, *Astron. Astrophys.*, 2009, **499**, 215–232.

5 F. J. Lovas, J. Hollis, A. J. Remijan and P. Jewell, *Astrophys. J.*, 2006, **645**, L137.

6 J. E. Elsila, J. P. Dworkin, M. P. Bernstein, M. P. Martin and S. A. Sandford, *Astrophys. J.*, 2007, **660**, 911.

7 A. Arnau, I. Tunon, E. Silla and J. Andres, *J. Chem. Educ.*, 1990, **67**, 905.

8 A. Belloche, R. T. Garrod, H. S. Muller and K. M. Menten, *Science*, 2014, **345**, 1584–1587.

9 B. Rowe, G. Dupeyrat, J. Marquette and P. Gaucherel, *J. Chem. Phys.*, 1984, **80**, 4915–4921.

10 B. Rowe, G. Dupeyrat, J. Marquette, D. Smith, N. Adams and E. Ferguson, *J. Chem. Phys.*, 1984, **80**, 241–245.

11 B. Rowe and J. Marquette, *Int. J. Mass Spectrom. Ion Processes*, 1987, **80**, 239–254.

12 I. W. Smith, *Chem. Soc. Rev.*, 2008, **37**, 812–826.

13 M. Fournier, S. D. Le Picard and I. R. Sims, 2017.

14 I. Sims, J. L. Queffelec, A. Defrance, C. Rebrion-Rowe, D. Travers, P. Bocherel, B. Rowe and I. W. Smith, *J. Chem. Phys.*, 1994, **100**, 4229–4241.

15 I. Sims, I. Smith, D. Clary, P. Bocherel and B. Rowe, *J. Chem. Phys.*, 1994, **101**, 1748–1751.

16 C. Sleiman, G. El Dib, D. Talbi and A. Canosa, *ACS Earth Space Chem.*, 2018.

17 D. B. Atkinson and M. A. Smith, *Rev. Sci. Instrum.*, 1995, **66**, 4434–4446.

18 J. M. Oldham, C. Abeysekera, B. Joalland, L. N. Zack, K. Prozument, I. R. Sims, G. B. Park, R. W. Field and A. G. Suits, *J. Chem. Phys.*, 2014, **141**, 154202.

19 C. Abeysekera, L. N. Zack, G. B. Park, B. Joalland, J. M. Oldham, K. Prozument, N. M. Ariyasingha, I. R. Sims, R. W. Field and A. G. Suits, *J. Chem. Phys.*, 2014, **141**, 214203.

20 O. Durif, M. Capron, J. P. Messinger, A. Benidar, L. Biennier, J. Bourgalais, A. Canosa, J. Courbe, G. A. Garcia and J.-F. Gil, *Rev. Sci. Instrum.*, 2021, **92**, 014102.

21 S. Soorkia, S. R. Leone and K. R. Wilson, 2012.

22 D. Chastaing, S. D. Le Picard and I. R. Sims, *J. Chem. Phys.*, 2000, **112**, 8466–8469.

23 S. S. Brown, A. Ravishankara and H. Stark, *J. Phys. Chem. A*, 2000, **104**, 7044–7052.

24 N. Suas-David, S. Thawoos and A. G. Suits, *J. Chem. Phys.*, 2019, **151**, 244202.

25 S. B. Morales, C. J. Bennett, S. D. Le Picard, A. Canosa, I. R. Sims, B. Sun, P. Chen, A. H. Chang, V. V. Kislov, A. M. Mebel, X. Gu, F. Zhang, P. Maksyutenko and R. I. Kaiser, *Astrophys. J.*, 2011, **742**, 26.

26 M. T. Butterfield, T. Yu and M. Lin, *Chem. Phys.*, 1993, **169**, 129–134.

27 A. Jamal and A. M. Mebel, *J. Phys. Chem. A*, 2013, **117**, 741–755.

28 A. Gardez, G. Saidani, L. Biennier, R. Georges, E. Hugo, V. Chandrasekaran, V. Roussel, B. Rowe, K. Reddy and E. Arunan, *Int. J. Chem. Kinet.*, 2012, **44**, 753–766.

29 C. Abeysekera, B. Joalland, Y. Shi, A. Kamasah, J. M. Oldham and A. G. Suits, *Rev. Sci. Instrum.*, 2014, **85**, 116107.

ART ■ D3FD00029J

30 M. Hippler and M. Quack, *Chem. Phys. Lett.*, 1999, **314**, 273–281.
31 P. Birza, T. Motylewski, D. Khoroshev, A. Chirokolava, H. Linnartz and J. Maier, *Chem. Phys.*, 2002, **283**, 119–124.
32 T. Motylewski and H. Linnartz, *Rev. Sci. Instrum.*, 1999, **70**, 1305–1312.
33 H. Verbraak, A. Ngai, S. Persijn, F. Harren and H. Linnartz, *Chem. Phys. Lett.*, 2007, **442**, 145–149.
34 J. Van Helden, R. Peverall, G. Ritchie, G. Berden and R. Engeln, *Cavity enhanced techniques using continuous wave lasers*, Wiley-Blackwell, West Sussex, UK, 2009.
35 J. A. Russell, I. A. McLaren, W. M. Jackson and J. B. Halpern, *J. Phys. Chem.*, 1987, **91**, 3248–3253.
36 C. Huang, W. Li, R. Silva and A. G. Suits, *Chem. Phys. Lett.*, 2006, **426**, 242–247.
37 W. Fisher, R. Eng, T. Carrington, C. Dugan, S. Filseth and C. Sadowski, *Chem. Phys.*, 1984, **89**, 457–471.
38 I. Nadler, H. Reisler and C. Wittig, *Chem. Phys. Lett.*, 1984, **103**, 451–457.
39 K. Kanda, S. Katsumata, T. Nagata, Y. Ozaki, T. Kondow, K. Kuchitsu, A. Hiraya and K. Shobatake, *Chem. Phys.*, 1993, **175**, 399–411.
40 S. Hay, F. Shokoohi, S. Callister and C. Wittig, *Chem. Phys. Lett.*, 1985, **118**, 6–11.
41 Y. Georgievskii and S. J. Klippenstein, *J. Phys. Chem. A*, 2003, **107**, 9776–9781.
42 E. E. Greenwald, S. W. North, Y. Georgievskii and S. J. Klippenstein, *J. Phys. Chem. A*, 2007, **111**, 5582–5592.
43 C. Cavallotti, M. Pelucchi, Y. Georgievskii and S. J. Klippenstein, *J. Chem. Theory Comput.*, 2019, **15**, 1122–1145.
10 44 C. Cavallotti, *Proc. Combust. Inst.*, 2022, **39**.
45 S. J. Klippenstein and C. Cavallotti, in *Computer Aided Chemical Engineering*, Elsevier, 2019, vol. 45, pp. 115–167.
46 B. Hanamirian, A. Della Libera, L. Pratali Maffei and C. CCavallotti, *J. Phys.*
11 *Chem. A*, 2003.
47 M. Frisch, G. Trucks, H. Schlegel, G. Scuseria, M. Robb, J. Cheeseman,
12 G. Scalmani, V. Barone, B. Mennucci and G. Petersson, Gaussian Inc, 2013.
48 H. J. Werner, P. J. Knowles, F. R. Manby, J. A. Black, K. Doll, A. Hesselmann, D. Kats, A. Kohn, T. Korona, D. A. Kreplin, Q. Ma, T. F. Miller 3rd, A. Mitrushchenkov, K. A. Peterson, I. Polyak, G. Rauhut and M. Sibaev, *J. Chem. Phys.*, 2020, **152**, 144107.
49 Y. Georgievskii, J. A. Miller, M. P. Burke and S. J. Klippenstein, *J. Phys. Chem. A*, 2013, **117**, 12146–12154.
50 S. B. Morales, S. D. Le Picard, A. Canosa and I. R. Sims, *Faraday Discuss.*, 2010, **147**, 155–171.
51 B. Sun, C. Huang, S. Chen, S. Chen, R. Kaiser and A. Chang, *J. Phys. Chem. A*, 2014, **118**, 7715–7724.
52 M. C. McCarthy and B. A. McGuire, *J. Phys. Chem. A*, 2021, **125**, 3231–3243.
53 K. K. Singh, P. Tandon, A. Misra, M. Yadav and A. Ahmad, *Int. J. Astrobiol.*, 2021, **20**, 62–72.
54 V. Vuitton, R. V. Yelle, S. J. Klippenstein, S. M. Hörst and P. Lavvas, *Icarus*, 2019, **324**, 120–197.
55 J. Loison, E. Hébrard, M. Dobrijevic, K. Hickson, F. Caralp, V. Hue, G. Gronoff, O. Venot and Y. Bénilan, *Icarus*, 2015, **247**, 218–247.
56 S. M. Hörst, *J. Geophys. Res.: Planets*, 2017, **122**, 432–482.

57 S. M. Hörst, C. He, N. K. Lewis, E. M.-R. Kempton, M. S. Marley, C. V. Morley, J. I. Moses, J. A. Valenti and V. Vuitton, *arXiv*, 2018, preprint, arXiv:1801.06512.
58 C. He, M. Radke, S. E. Moran, S. M. Horst, N. K. Lewis, J. I. Moses, M. S. Marley, N. E. Batalha, E. M.-R. Kempton and C. V. Morley, *arXiv*, 2023, preprint, arXiv:2301.02745.
59 C. Ennis, M. L. Cable, R. Hodyss and H. E. Maynard-Casely, *ACS Earth Space Chem.*, 2020, **4**, 1195–1200.
60 M. L. Cable, T. e. Runčevski, H. E. Maynard-Casely, T. H. Vu and R. Hodyss, *Acc. Chem. Res.*, 2021, **54**, 3050–3059.
61 R. Garrod, A. Belloche, H. Müller and K. Menten, *Astron. Astrophys.*, 2017, **601**, A48.
62 A. Belloche, R. Garrod, O. Zingsheim, H. Müller and K. Menten, *Astron. Astrophys.*, 2022, **662**, A110.

ART ■ D3FD00029J